Spontaneous Resolution of Chiral Multi-Thiolate-Protected Ag_{30} nanoclusters

Jia-Hong Huang[1], Zhao-Yang Wang[1,*], Shuang-Quan Zang[1,3,*] and Thomas C. W. Mak[2]

[1]*Green Catalysis Center, and College of Chemistry, Zhengzhou University, Zhengzhou 450001, China.*

[2]*Department of Chemistry, The Chinese University of Hong Kong, Shatin, New Territories, Hong Kong SAR, China.*

* Correspondence: zangsqzg@zzu.edu.cn;

wangzy@zzu.edu.cn

Experimental Section

Materials and reagents. Silver nitrate ($AgNO_3$), trifluoroacetic acid, sodium borohydride ($NaBH_4$, 98.0%), bis(diphenylphosphino)methane and hydrazine hydrate (80%) were purchased from Aladdin. All reagents and solvents were used directly as received without further purification. 8,9,12-Trimercapto-1,2-closo-carborane was prepared according to the literature method[1] and characterized by ^{1}H NMR spectrum (Figure S17). No unexpected or unusually high safety hazards were encountered.

Characterizations. ^{1}H NMR spectra were recorded on a Bruker DRX spectrometer operating at 400 MHz. Powder X-ray diffraction (PXRD) patterns of $Ag_{30}(C_2B_{10}H_9S_3)_8$ were collected using a Rigaku MiniFlex600 diffractometer (Cu Kα, λ = 1.54178 Å). X-ray photoelectron spectroscopy (XPS) was recorded using Thermo ESCALAB 250XI with Al *K*α as excitation source. Binding energy were calibrated by C 1s at 284.8 eV. ESI-TOF-MS was measured on a X500R QTOF spectrometer. UV/Vis absorption spectra were recorded in the range of 200-800 nm using an U-2000 UV-visible spectrophotometer. Steady- and transient state photoluminescence (PL) spectra were carried out at room temperature with a HORIBA FluoroLog-3 fluorescence spectrometer. Circularly polarized luminescence (CPL) spectra were measured on an JASCO CPL-300 equipment.

Single-Crystal X-ray Diffraction Analysis (SCXRD). SCXRD measurements were performed on a Rigaku XtaLAB Pro diffractometer with Cu- Kα radiation (λ = 1.54184 Å) at 200 K for **Ag$_{30}$-*rac***, 100 K for ***L*-Ag$_{30}$** and ***R*-Ag$_{30}$**. Data collection and reduction were performed using the program CrysAlisPro.[2] The intensities were corrected for absorption using empirical method implemented in SCALE3 ABSPACK scaling algorithm. The structures were solved with intrinsic phasing methods (*SHELXT-2015*),[3] and refined by full-matrix least squares on F^2 using *OLEX2*,[4] which utilizes the *SHELXL-2015* module.[3] All non-hydrogen atoms were refined anisotropically, and the hydrogen atoms were included on idealized positions. SQUEEZE option of PLATON was used at the final refinement to account for the contribution of disordered solvent molecules to the calculated structure factors.[5] The crystal structures are visualized by DIAMOND 3.2.[6]

Synthesis and chiral self-resolution of Ag$_{30}$-*rac*.
8,9,12-Trimercapto-1,2-closo-carborane (4.8 mg) and CF_3COOAg (13.2 mg) were successively added to 4 mL acetonitrile to form a turbid yellow suspension. Then Dppm (9.0 mg) was added to the resultant suspension to afford a transparent yellow solution within several minutes. Subsequently, 20 μL hydrazine hydrate (80%) was added in one portion under vigorous stirring, and the solution turned yellow and became turbid immediately. The reaction mixture was kept for 12 h in the dark. The resultant yellow suspension was centrifuged to isolate the microcrystalline **Ag$_{30}$-*rac*** from the yellow supernatant. The supernatant was evaporated slowly and yielded yellow block-like crystals of **Ag$_{30}$-*rac*** suitable for single-crystal X-ray diffraction. Collective yield: *ca*. 65% (based on Ag). The pure **Ag$_{30}$-*rac*** collected sample was recrystallized in DMAc by slow evaporation for two weeks to afford yellow prism-like crystals of ***R*/*L*-Ag$_{30}$** in a yield of *ca*. 50%.

Supplementary Figures and Tables

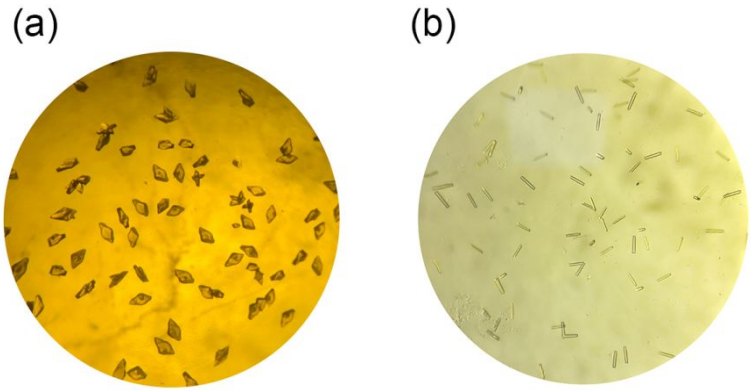

Figure S1. Photographs for crystals of (a) **Ag_{30}-*rac***, (b) ***R/L*-Ag_{30}**.

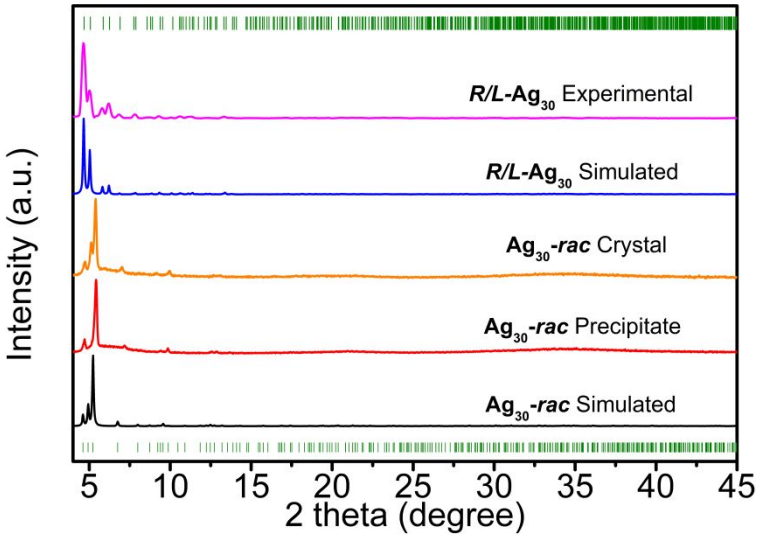

Figure S2. PXRD patterns of **Ag_{30}-*rac*** and ***R/L*-Ag_{30}**.

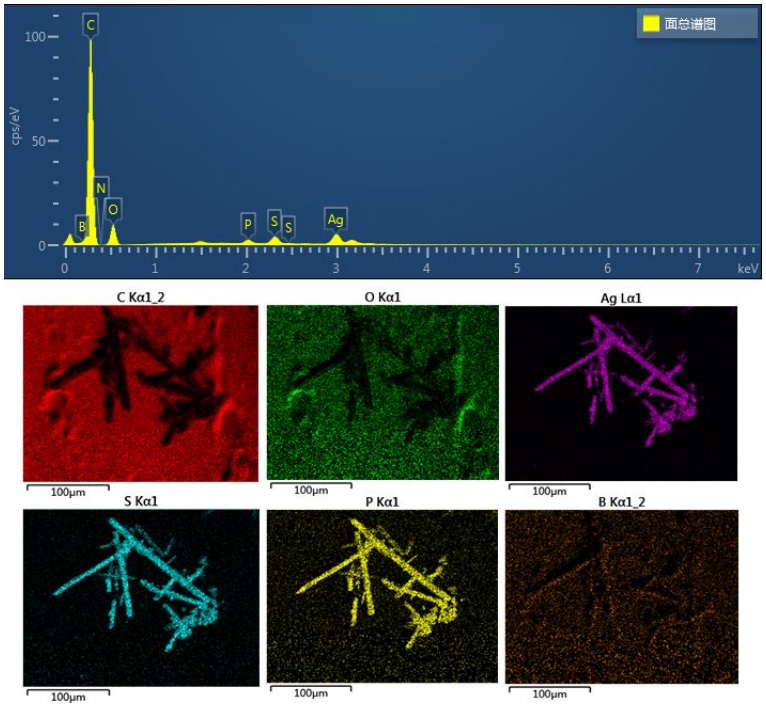

Figure S3. Energy dispersive spectroscopy (EDS) mapping results of the ***R/L*-Ag$_{30}$**.

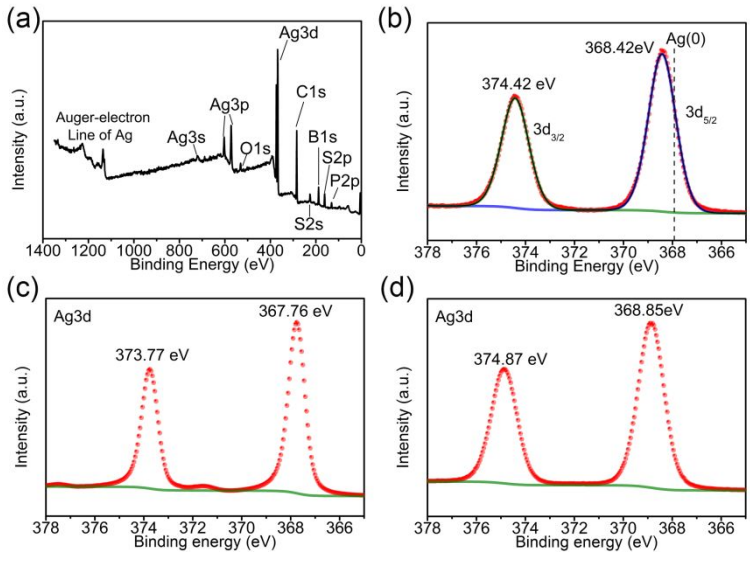

Figure S4. XPS survey scan of **Ag$_{30}$-*rac*** (a) and Ag 3d XPS spectra of **Ag$_{30}$-*rac*** (b), Ag(0) powder (c), CF_3COOAg (d).

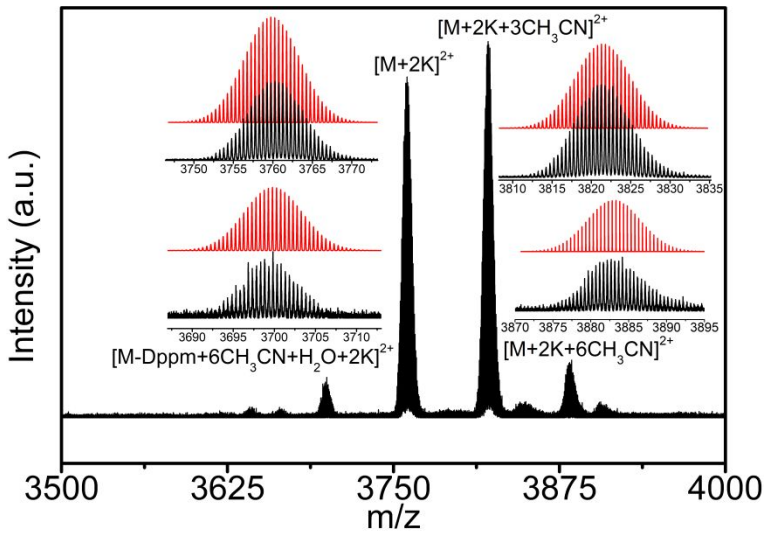

Figure S5. Positive-ion ESI-MS spectrum of **Ag_{30}-*rac*** in a mixed DMF, THF and CH_3CN. Inset: Enlarged portion of the spectrum showing the measured (black) and simulated (red) isotopic distribution patterns (M = $Ag_{30}(C_2B_{10}H_9S_3)_8Dppm_6$).

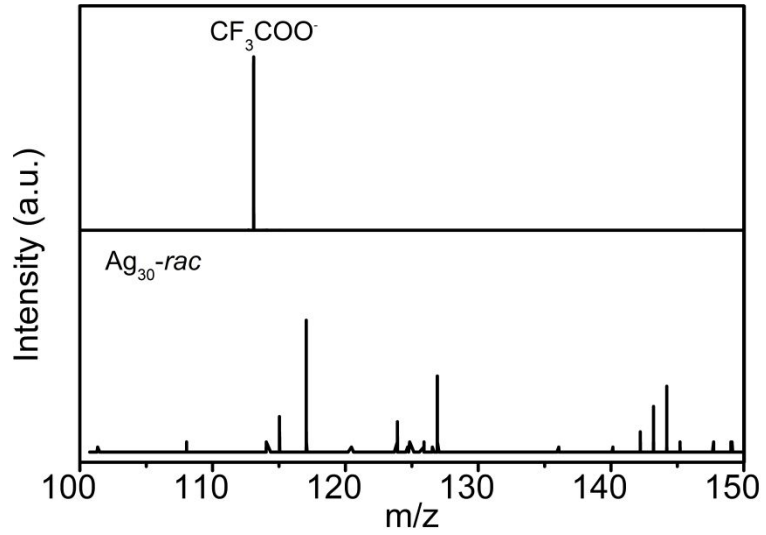

Figure S6. The negative-ion ESI-MS spectrum of **Ag_{30}-*rac*** in a mixed solvent of DMF, THF and CH_3CN in comparison to CF_3COO^-.

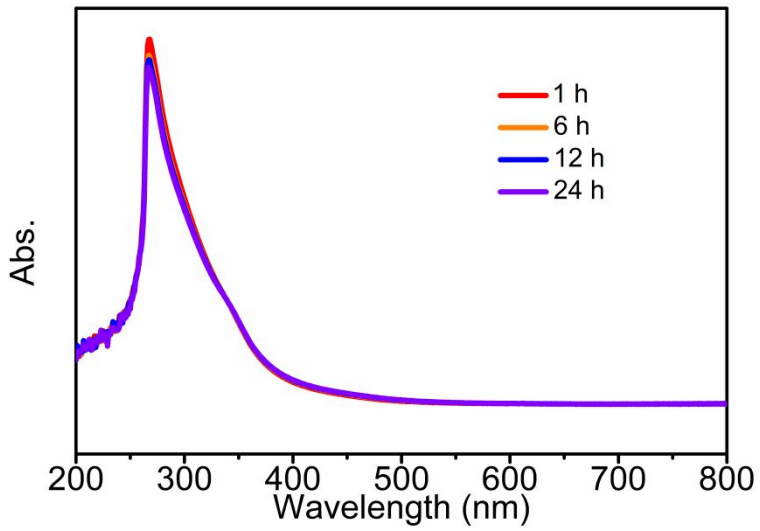

Figure S7. The time-dependent UV-vis absorption spectra of **Ag_{30}-*rac*** in DMAc.

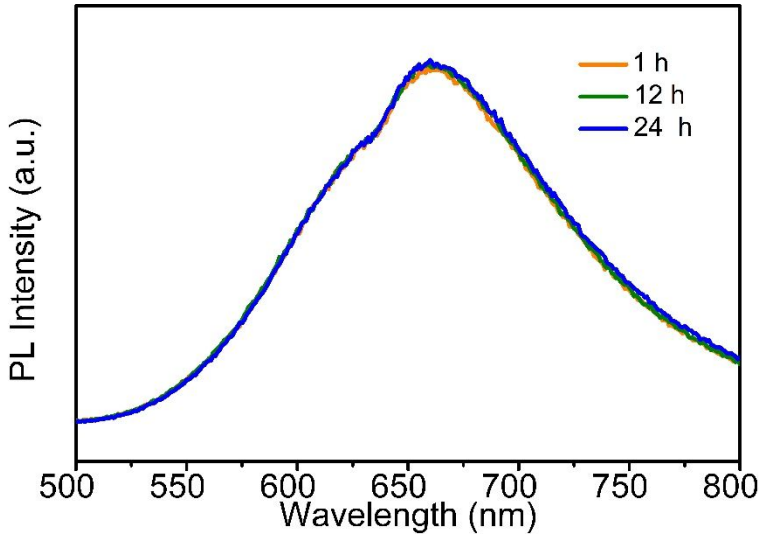

Figure S8. Time-dependent luminescent spectra of **Ag_{30}-*rac*** in DMAc.

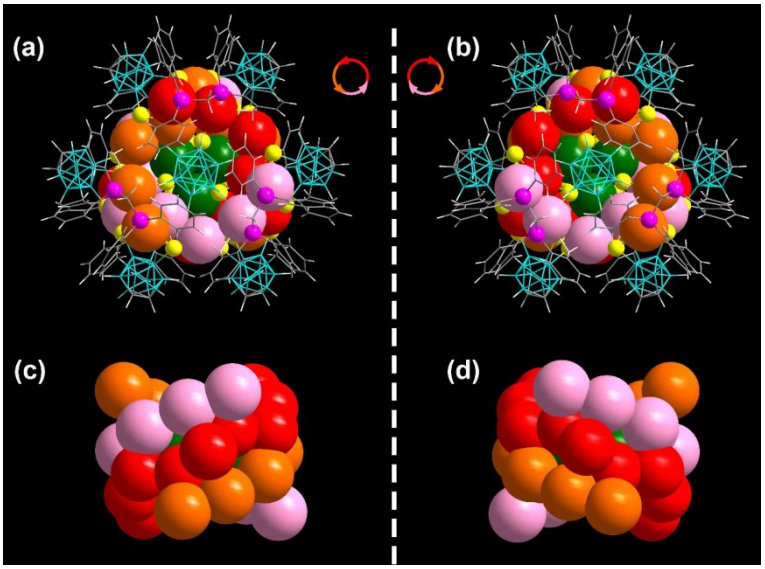

Figure S9. (a) (b) Overall structure of the enantiomers in **Ag_{30}-*rac*** viewed from the top. (c) (d) Arrangements of Ag atoms viewed from the side. Color labels: green, red, orange and light pink, Ag; yellow, S; pink, P; gray, C; cyan, B; white, H.

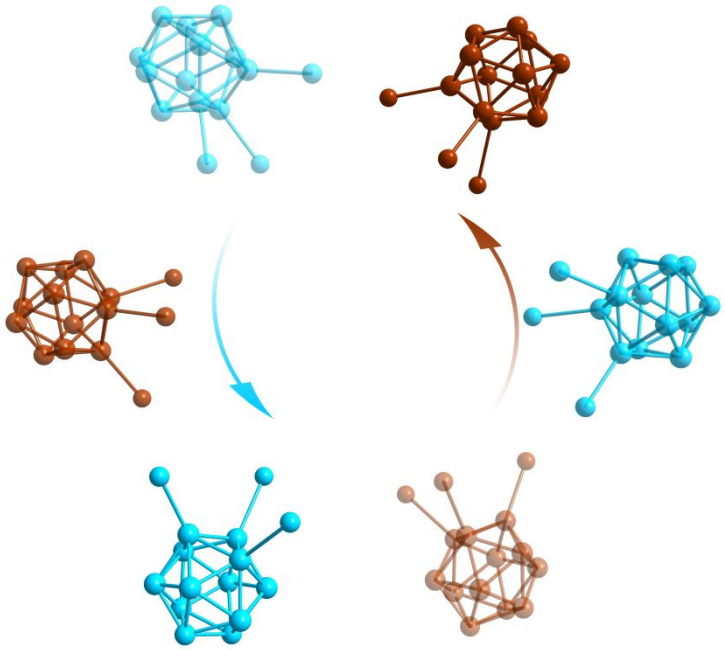

Figure S10. Two sets of chiral arranged carboranetrithiolates anchoring on the waist of the Ag_{30} nanocluster.

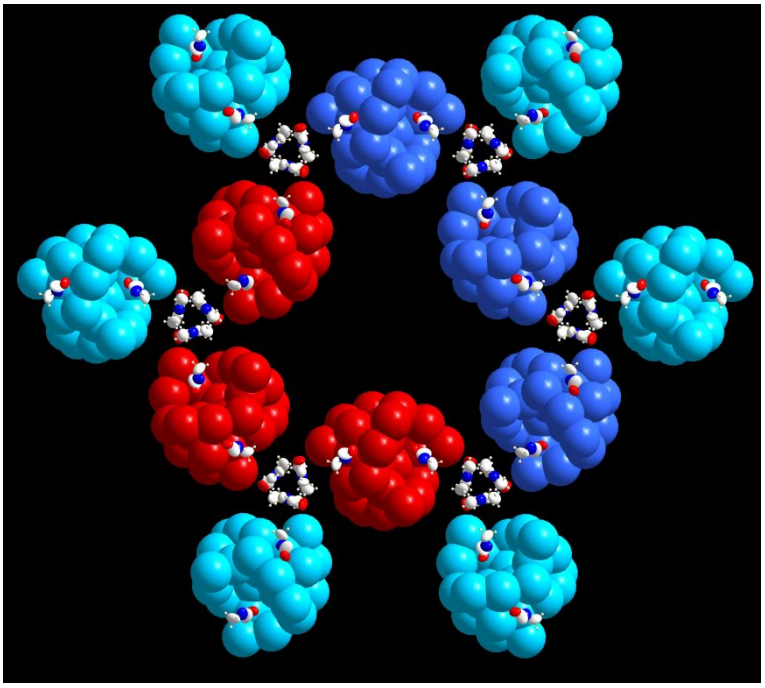

Figure S11. The arrangement of DMAc molecules in the lattice. Color labels: cyan, blue, and deep red, Ag; blue, N; red, O; white, H.

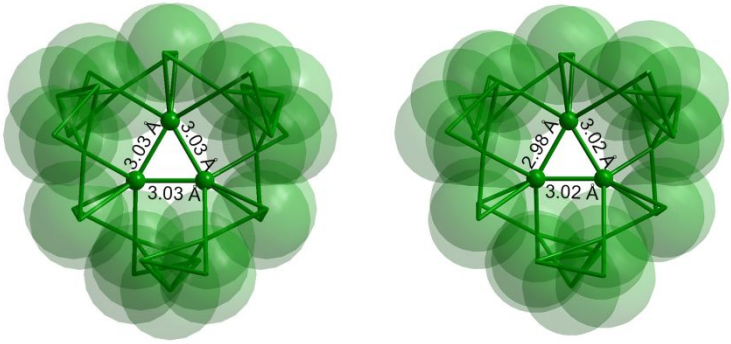

Figure S12. Metal framework of the nanocluster in **Ag_{30}-*rac*** (left) and ***R/L*-Ag_{30}** (right).

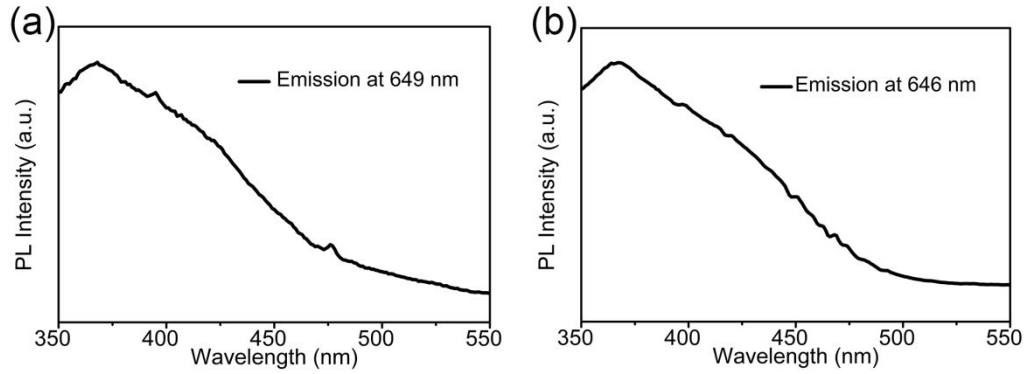

Figure S13. The excitation spectra of **Ag_{30}-*rac*** (left) and ***R/L*-Ag_{30}** (right).

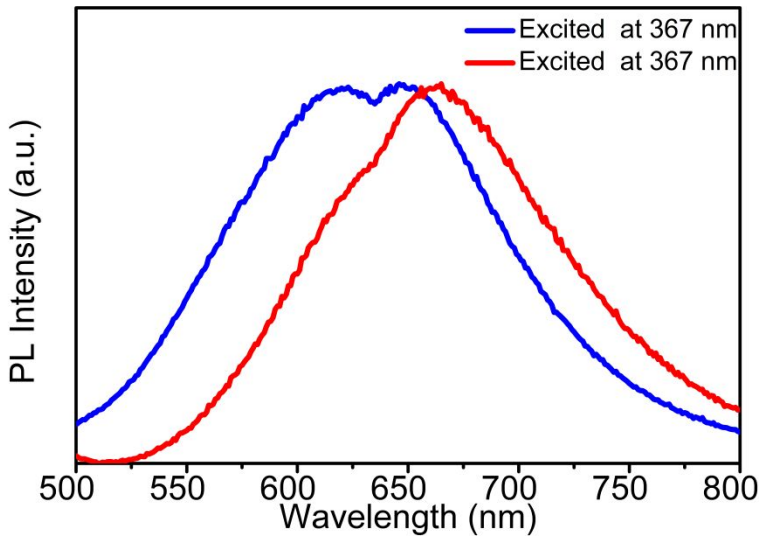

Figure S14. Photoluminescence (PL) spectra of **Ag_{30}-*rac*** in the solid state (blue line) and in DMAc solution (red line).

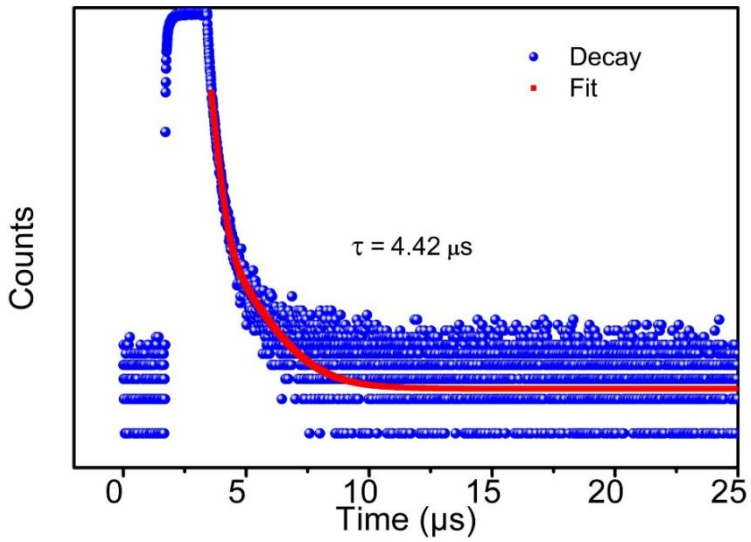

Figure S15. Decay times of **Ag_{30}-*rac*** in the solid state at room temperature.

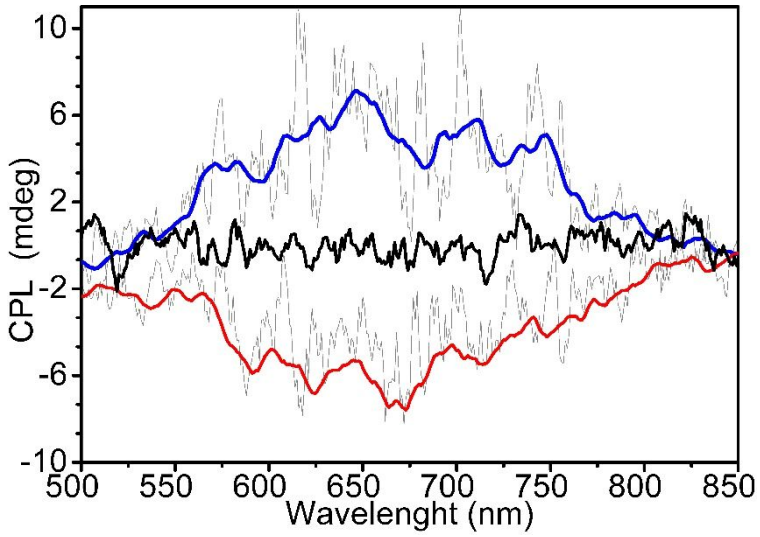

Figure S16. CPL spectra of ***R*-Ag_{30}** (red), ***L*-Ag_{30}** (blue) and **Ag_{30}-*rac*** (black).

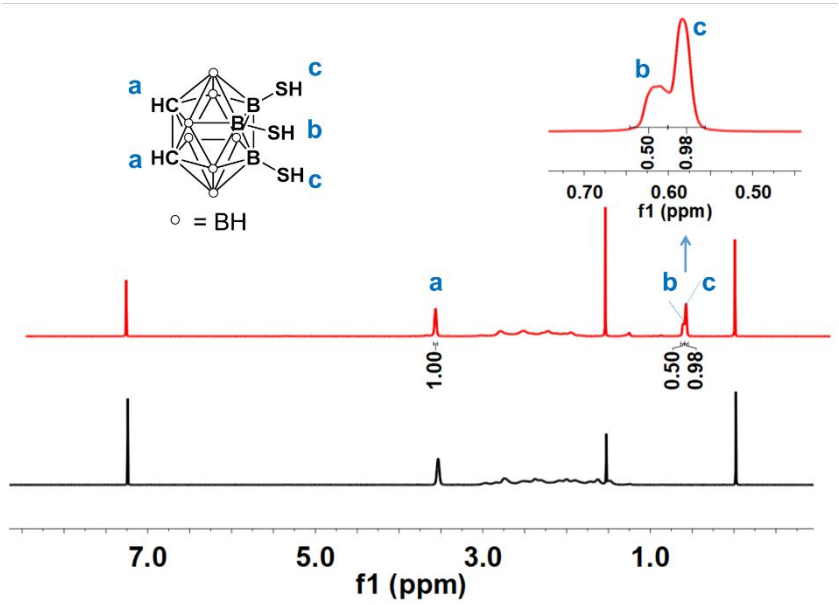

Figure S17. ^{1}H-NMR ($CDCl_3$) spectrum of 8,9,12-trimercapto-1,2-closo-carborane (red line) and 1,2-closo-carborane (black line).

Supplementary Table 1. Crystal and structure determination data

Identification code	Ag_{30}-*rac*	*R*-Ag_{30}	*L*-Ag_{30}
CCDC number	2010140	2010153	2010157
Empirical formula	$C_{166}H_{204}Ag_{30}B_{80}P_{12}S_{24}$	$C_{182}H_{240}Ag_{30}B_{80}N_4O_4P_{12}S_{24}$	$C_{182}H_{240}Ag_{30}B_{80}N_4O_4P_{12}S_{24}$
Formula weight	7441.11	7789.75	7789.75
Temperature/K	200.00(10)	100.00(2)	100.00(10)
Crystal system	trigonal	trigonal	trigonal
Space group	*P*-31*c*	$P3_221$	$P3_121$
a/Å	22.084(2)	34.9242(3)	34.8668(13)
b/Å	22.084(2)	34.9242(3)	34.8668(13)
c/Å	35.768(1)	24.1417(2)	24.0968(6)
α/°	90	90	90
β/°	90	90	90
γ/°	120	120	120
Volume/Å^3	15107(2)	25500(5)	25370(2)
Z	2	3	3
ρ_{calc}g/cm^3	1.636	1.522	1.530
μ/mm^{-1}	17.61	15.689	15.77
F(000)	7148	11298	11298
Crystal size/mm^3	0.15 × 0.17 × 0.2	0.12 × 0.08 × 0.06	0.15 × 0.05 × 0.05
Radiation	Cu Kα (λ = 1.54184)	Cu Kα (λ = 1.54184)	Cu Kα (λ = 1.54184)
2Θ range for data collection/°	4.62 to 124.994	4.684 to 129.996	5.854 to 130.996
Index ranges	-25 ≤ h ≤ 24, -25 ≤ k ≤ 21, -34 ≤ l ≤ 41	-22 ≤ h ≤ 41, -40 ≤ k ≤ 20, -26 ≤ l ≤ 28	-28 ≤ h ≤ 39, -41 ≤ k ≤ 41, -14 ≤ l ≤ 28
Reflections collected	44730	81938	81583
Independent reflections	8046 [R_{int} = 0.1607, R_{sigma} = 0.1019]	28183 [R_{int} = 0.0432, R_{sigma} = 0.0491]	28374 [R_{int} = 0.1020, R_{sigma} = 0.0952]
Data/restraints/parameters	8046/1214/422	28183/228/1487	28374/1392/1426
Goodness-of-fit on F^2	1.179	0.953	0.929
Final R indexes [I>=2σ (I)]	R_1 = 0.1137, wR_2 = 0.3578	R_1 = 0.0481, wR_2 = 0.1217	R_1 = 0.0793, wR_2 = 0.192
Final R indexes [all data]	R_1 = 0.1551, wR_2 = 0.3837	R_1 = 0.0624, wR_2 = 0.1288	R_1 = 0.1286, wR_2 = 0.2287
Largest diff. peak/hole / e Å^{-3}	1.02/-0.84	0.87/-0.66	1.32/-0.94
Flack parameter	–	0.012(4)	0.017(8)

Reference:

(1) Zhang, X., Tang, X., Yang, J., Li, Y., Yan, H. and Bregadze, V. I. *Organometallics* **2013**, *32*, 2014-2018.
(2) CrysAlisPro 2012, Agilent Technologies. Version 1.171.36.31.
(3) Sheldrick, G. M. *Acta Cryst. A* **2015**, *71*, 3-8.
(4) Dolomanov, O. V.; Bourhis, L. J.; Gildea, R. J.; Howard, J. A. K.; Puschmann, H. *J. Appl. Cryst.* **2009**, *42*, 339-341.
(5) Spek, A. L. *Acta Cryst. C* **2015**, *71*, 9-18.
(6) Brandenburg, K. Diamond, **2010**.